

Experimental investigation of adsorption water desalination/cooling system using CPO-27Ni MOF

Youssef, Peter George; Dakkama, Hassan; Mahmoud, Saad; Al-Dadah, Raya

DOI:

[10.1016/j.desal.2016.11.008](https://doi.org/10.1016/j.desal.2016.11.008)

License:

Creative Commons: Attribution-NonCommercial-NoDerivs (CC BY-NC-ND)

Document Version

Peer reviewed version

Citation for published version (Harvard):

Youssef, PG, Dakkama, H, Mahmoud, S & Al-Dadah, R 2017, 'Experimental investigation of adsorption water desalination/cooling system using CPO-27Ni MOF', *Desalination*, vol. 404, pp. 192-199.

<https://doi.org/10.1016/j.desal.2016.11.008>

[Link to publication on Research at Birmingham portal](#)

General rights

Unless a licence is specified above, all rights (including copyright and moral rights) in this document are retained by the authors and/or the copyright holders. The express permission of the copyright holder must be obtained for any use of this material other than for purposes permitted by law.

- Users may freely distribute the URL that is used to identify this publication.
- Users may download and/or print one copy of the publication from the University of Birmingham research portal for the purpose of private study or non-commercial research.
- User may use extracts from the document in line with the concept of 'fair dealing' under the Copyright, Designs and Patents Act 1988 (?)
- Users may not further distribute the material nor use it for the purposes of commercial gain.

Where a licence is displayed above, please note the terms and conditions of the licence govern your use of this document.

When citing, please reference the published version.

Take down policy

While the University of Birmingham exercises care and attention in making items available there are rare occasions when an item has been uploaded in error or has been deemed to be commercially or otherwise sensitive.

If you believe that this is the case for this document, please contact UBIRA@lists.bham.ac.uk providing details and we will remove access to the work immediately and investigate.

Experimental Investigation of Adsorption Water Desalination/Cooling System Using CPO-27Ni MOF

Peter G. Youssef*, Hassan Dakkama, Saad M. Mahmoud, Raya K. AL-Dadah

Abstract — Although many adsorbent materials have been used in adsorption systems, only silica-gel was tested experimentally for desalination applications. This work experimentally and numerically investigates the use of CPO-27(Ni) an advanced Metal Organic Framework-MOF adsorbent material in a 1-bed adsorption system for water desalination and cooling applications. Operating parameters as switching time, half cycle time, evaporator and condenser water inlet temperatures were studied to investigate their effects on cycle water production and cooling. Moreover, a mathematical simulation model is developed, validated and used to predict cycle outputs at other operating conditions. Results showed that as evaporator temperature increases and condenser temperature decreases, cycle outputs increase. Also, it was shown that adsorption desalination cycles can work with condenser pressure lower than evaporator pressure as the cycle is an open loop one (i.e. no refrigerant is flowing back from condenser to evaporator). A water production of 22.8m³/tonne.ads/day was achieved using 40°C evaporator temperature, 5°C condenser temperature and 95°C desorption temperature. Similar water production can be achieved using 30°C condensing temperature but at 120°C desorption temperature. For space cooling applications ($T_{\text{evap}} < 20^\circ\text{C}$), cycle cooling produced was found to be 65Rton/tonne.ads. This work highlights the potential of using advanced MOF materials for water desalination/ cooling applications.

Keywords—Experimental, Adsorption, CPO-27(Ni), Desalination, Cooling, Seawater.

1. INTRODUCTION

Many countries depend on water desalination technologies to meet their potable water needs. Four water desalinating techniques are widely used which are reverse osmosis (RO), multistage flash (MSF), multi-effect distillation (MED) and mechanical vapor compression (MVC) [1]. However, these techniques suffer from high power consumption which in turn increases CO₂ emissions and water production costs [2, 3]. Recently adsorption desalination technology was reported to outperform the current conventional technologies in terms of high grade fresh potable water of salinity as low as 10 ppm, lower electric energy consumption of 1.38kWh/m³ and CO₂ emission of 0.6kg/m³ while having lower water production cost of 0.2\$/m³ [4].

Nomenclature

c_p	Specific heat at constant pressure (kg. kg ⁻¹ .K ⁻¹)	$SDWP$	Specific daily water production (m ³ t ⁻¹ day ⁻¹)
h	Enthalpy (kJ.kg ⁻¹)	T	Temperature (K)
M	Mass (kg)	W	Uptake (kg.kg ⁻¹)
m	Mass flow rate (kg.s ⁻¹)	W^*	Equilibrium uptake (kg. kg ⁻¹)
n	Adsorption/Desorption phase, flag (-)	X	Salt concentration (ppm)
P	Pressure (kPa)	θ	Seawater charging flag (-)
Q_{st}	Isosteric heat of adsorption (kJ/kg)	γ	Brine discharge flag (-)
SCP	Specific cooling power (Rton/t ⁻¹)	τ	No of cycles per day (-)

Subscripts

a	Adsorbent material	f	Liquid
ads	Adsorption	hw	Heating Water
b	Brine	HX	Heat exchanger
$cond$	Condenser	in	inlet
cw	Cooling Water	ads	adsorber bed
D	vapor	des	desorber bed
d	Distillate water	out	outlet
des	Desorption	s	Seawater
$evap$	Evaporator	t	Time

The adsorption water desalination cycle consists of three main components namely adsorption/desorption bed, evaporator and condenser producing desalinated water (from condenser) and cooling (from evaporator) [5-9]. The desalination/refrigeration adsorption system depends on the combination of four processes; evaporation due to adsorption and condensation as a result of desorption. Seawater is fed into the evaporator where it is evaporated as a result of the associated adsorption process while extracting heat from the chilled water passing through the evaporator coil producing the cooling effect in this cycle [6, 10]. In the adsorption process, water vapour is adsorbed by the adsorbent material while in the desorption process the water vapour is regenerated by heating and the desorbed water vapour is then condensed in the condenser producing fresh water [11, 12].

Different adsorbent materials including silica-gel and zeolite have been reported for desalination applications using different cycle configurations. Thu et al. [13] experimentally tested an adsorption desalination system operates in two and four bed modes. Heating source temperature and cycle time have

43 been examined during their tests for the two operating modes. It was found that as heat source temperature
44 decreases, longer cycle time is required to obtain the highest water production. In addition, in two bed
45 mode, maximum water production reported was 8.7 m³/tonne of silica-gel/day when 85°C hot source
46 temperature was used while for four bed mode, at the same heating temperature, 10 m³/tonne of silica-
47 gel/day was produced.

48 Ng et al. [8], have used a 215 m² solar collector to obtain the required heating for regeneration of water
49 vapor in a 2 bed silica-gel adsorption system for water desalination and cooling applications. The solar
50 collector produced heat source temperature varying from 65 to 80°C which used to produce 3-5 m³ of
51 desalinated water and cooling in the range of 25-35 Rton/tonne of silica-gel at chilled water temperature of
52 7 to 10°C.

53 Mitra et al. [14], have introduced a new adsorption cycle for desalination and cooling. This system has 2
54 stages with 2 beds per stage. Simulations as well as experiments have been carried out at different
55 evaporator pressures and half cycle times to predict desalinated water output, cooling capacity and
56 coefficient of performance (COP). Results showed that maximum produced desalinated water is 1 m³/tonne
57 silica-gel/day while cooling capacity is 7.5 Rton/tonne silica-gel with COP value of 0.25. These results
58 were obtained at evaporator pressure of 1.7 kPa and half cycle time of 1800 sec. The authors attributed
59 these low production capacities, compared to literature, to the quite high ambient temperature, 41°C, which
60 affected the performance of the air cooled condenser. In addition, 2-3 times larger silica gel particle sizes
61 than those reported in literature were used which resulted in slower adsorption/desorption rates.

62 Youssef et al. [15], have studied the use of advanced zeolite material, AQSOA-ZO2, for adsorption
63 desalination and cooling applications. In their work, a comparison between the AQSOA-ZO2 and silica-gel
64 has been performed when operating in a two bed adsorption cycle for the production of desalinated water
65 and cooling. The key parameters of the comparison are SDWP and specific cooling power (SCP) while
66 different heating source temperatures and evaporator water inlet temperatures were applied. It was found
67 that AQSOA-ZO2 is less sensitive than silica gel to evaporator water temperature variations. Accordingly,
68 AQSOA-ZO2 outperformed silica-gel at lower evaporator water temperatures less than 25°C where at 10°C
69 evaporator water temperature, AQSOA-ZO2 cycle can produce 5.8 m³ water per day and 50.1 Rton of
70 cooling while silica-gel cycle generate only SDWP of 2.8 m³ and SCP of 17.2 Rton. On the other hand, at
71 the same heating temperature of 85°C but at 30°C evaporator water temperature silica-gel cycle produces
72 maximum SDWP of 8.4 m³ and 62.4 Rton of cooling.

73 Youssef et al. [16], have investigated the use of AQSOA-ZO2 in a novel adsorption system consisting of
74 evaporator, condenser, integrated evaporator-condenser device and 4 adsorber beds. Results showed that by
75 utilizing heat recovery between system components, water production can reach 12.4 m³/tonne

76 adsorbent/day and cooling of 32.4 Rton/tonne adsorbent at evaporator inlet water temperature of 10°C.
77 Also, results showed that this system can produce 15.4 m³/tonne adsorbent/day of desalinated water if no
78 cooling is required.

79 Ali et al. [17], have presented a double stage system to produce cooling through stage-1 and desalinated
80 water from condensers of stages 1 and 2. AQSOA-Z02 and silica-gel were used as adsorbents in the two
81 stages, 1 and 2 respectively. A heat recovery was implemented between condensers and evaporators of the
82 system to reduce condenser pressure and increase evaporator pressure which resulted in increased cycle
83 outputs. Results showed that this new configuration produced more water by 26% and 45% more cooling
84 compared to the conventional adsorption desalination and cooling systems.

85 Elsayed et al. [18], have investigated numerically the potential of using two metal organic framework
86 adsorbent materials (MOF) for different adsorption applications including water desalination and cooling.
87 Isotherms, kinetics and cycle stability were measured for both CPO-27(Ni) and Aluminum fumarate MOF
88 materials where the maximum uptake was 0.47 and 0.53 kg_{water}/kg_{adsorbent} respectively. It was found that at
89 high desorption temperatures (>90°C) and low evaporation temperature (5°C), CPO-27(Ni) outperforms Al-
90 Fumarate. However, Al-Fumarate resulted in better performance at high evaporation temperature of 20°C
91 and/or low bed heating temperature of 70°C.

92 All reviewed work on water adsorption desalination, showed that silica-gel / water is the only working
93 pairs investigated experimentally. This work, experimentally investigates the use of an advanced metal
94 organic frameworks adsorbent material, (CPO-27Ni, produced by Johnson Matthey Ltd) in a 1 bed
95 adsorption cycle for production of fresh water and cooling. In addition, a numerical simulation is carried
96 out, validated and used to predict the system performance at other operating conditions.

97

98 **2. EXPERIMENTAL TEST FACILITY**

99 Figure 1 shows a schematic diagram for a lab scale adsorption test facility developed for the production
100 of fresh water and cooling using CPO-27Ni MOF material as an adsorbent. The main components of this
101 system are: adsorption bed, evaporator and condenser shown pictorially in figure 2.

102 In such adsorption water desalination system, seawater is supplied to the evaporator where it evaporates
103 during the adsorption half cycle while the adsorber bed is connected to the evaporator. During adsorption
104 time, cooling water is circulated in the adsorption bed to absorb the released heat from the adsorbent
105 material. Then, in the desorption phase, the bed is heated by hot water and water vapor is regenerated.
106 During this desorption process, the adsorber bed is connected to the condenser where the water vapour is
107 condensed producing fresh water. As shown in figure 2, there are other auxiliary components in the system

which are heating and cooling water systems for the bed and temperature controllers to supply constant water temperatures for the evaporator and condenser. In addition, there are vacuum pumps to generate the required vacuum pressure in the system. Adsorber bed as shown in figure 3 is a rectangular finned tube heat exchanger with the adsorbent material packed between the fins and surrounded by a metal mesh to keep adsorbent particles in position. The evaporator and condenser are cylindrical vacuum designed chambers with helically shaped cooling coil.

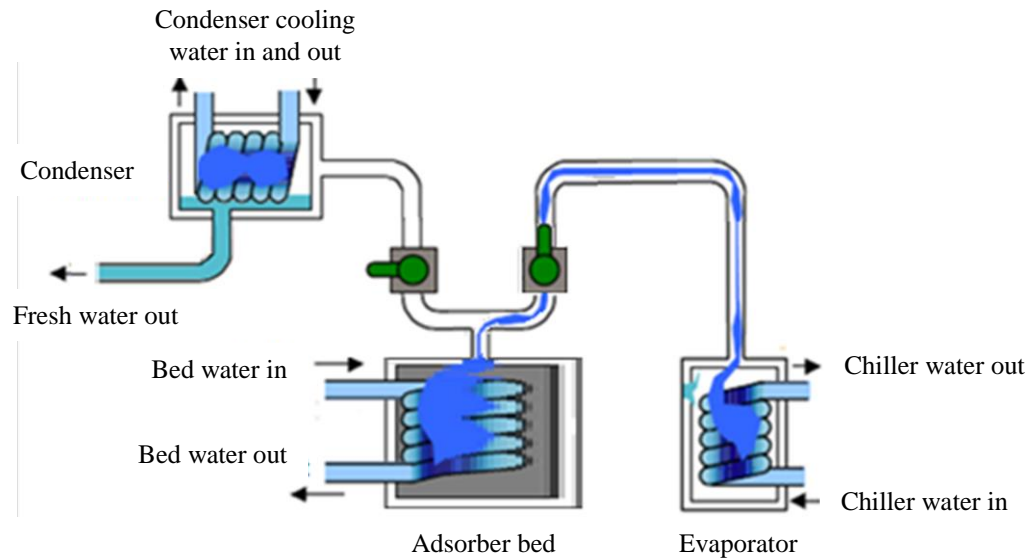


Fig. 1 Schematic diagram for a 1-bed adsorption

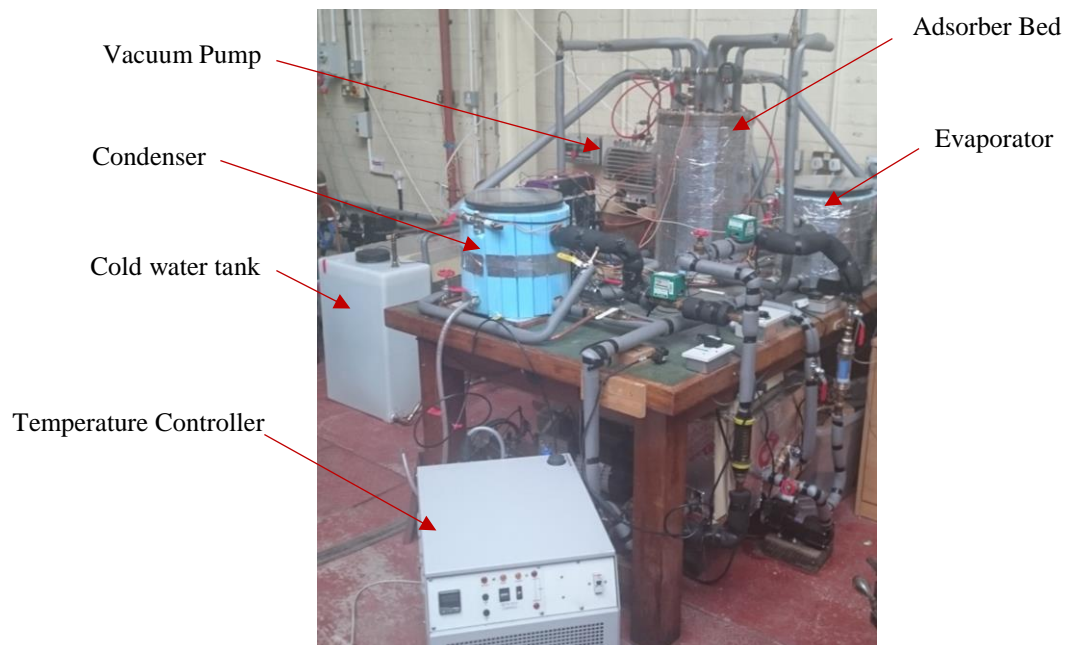


Fig. 2 Pictorial view for the single-bed adsorption test rig

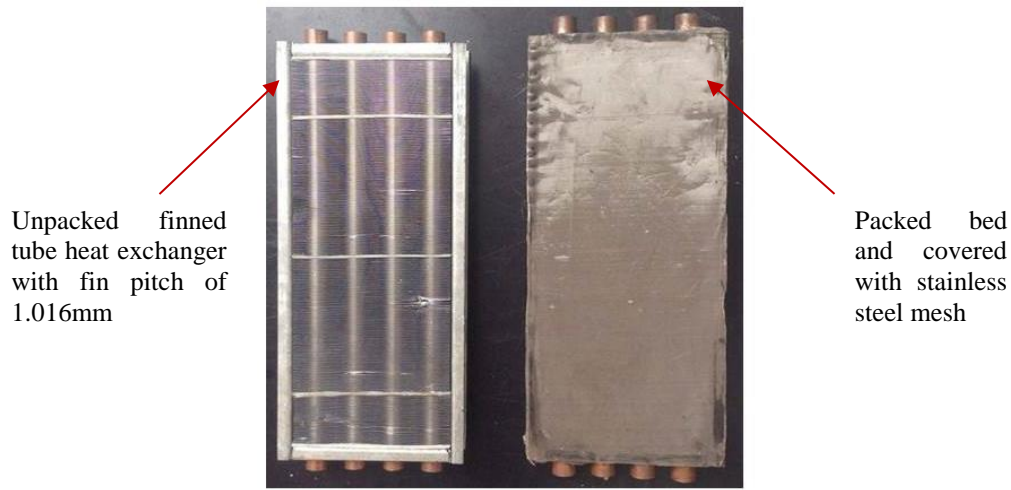


Fig. 3 Pictorial view for the adsorber bed

The experimental test facility is equipped with TJC100-CPSS T-type thermocouples to measure the temperature of the evaporator liquid and gas, adsorbent material in bed and vapor in the bed space. In the condenser, RS-pro, k-type thermocouples are used for measuring vapor and condensed water temperatures. Platinum RTD temperature sensors were used to measure bed heating and cooling water inlet and outlet temperatures, evaporator and condenser circulating water inlet and outlet temperatures. The evaporator, condenser and adsorber bed pressures are measured using pressure transducers with an accuracy of ± 0.01 kPa. Flowmeters of type FLC-H14 (0-57 LPM) are used to measure the adsorber bed heating/cooling water flowrate manually with an accuracy of ± 1 L while flowrates of condenser and evaporator water circuits are measured by Parker type flowmeter (2-30 LPM) with an accuracy of $\pm 5\%$. Details of the system component specifications and operating conditions are presented in table I.

TABLE I
System specifications

Property	Value
<i>System specifications</i>	
<i>Adsorbent mass</i>	0.67 kg
<i>Bed metal mass</i>	29.3 kg
<i>Evaporator metal mass</i>	15.1 kg
<i>Condenser metal mass</i>	15.1 kg
<i>Bed heat transfer area</i>	2.55 m ²
<i>Evaporator heat transfer area</i>	0.11 m ²
<i>Condenser heat transfer area</i>	0.16 m ²

3. ADSORBENT MATERIAL CHARACTERISTICS

CPO-27Ni used in this work is an MOF adsorbent manufactured commercially by Johnson Matthey. Figure 4 shows SEM image for this adsorbent material and its physical properties are listed in table II [19-21]

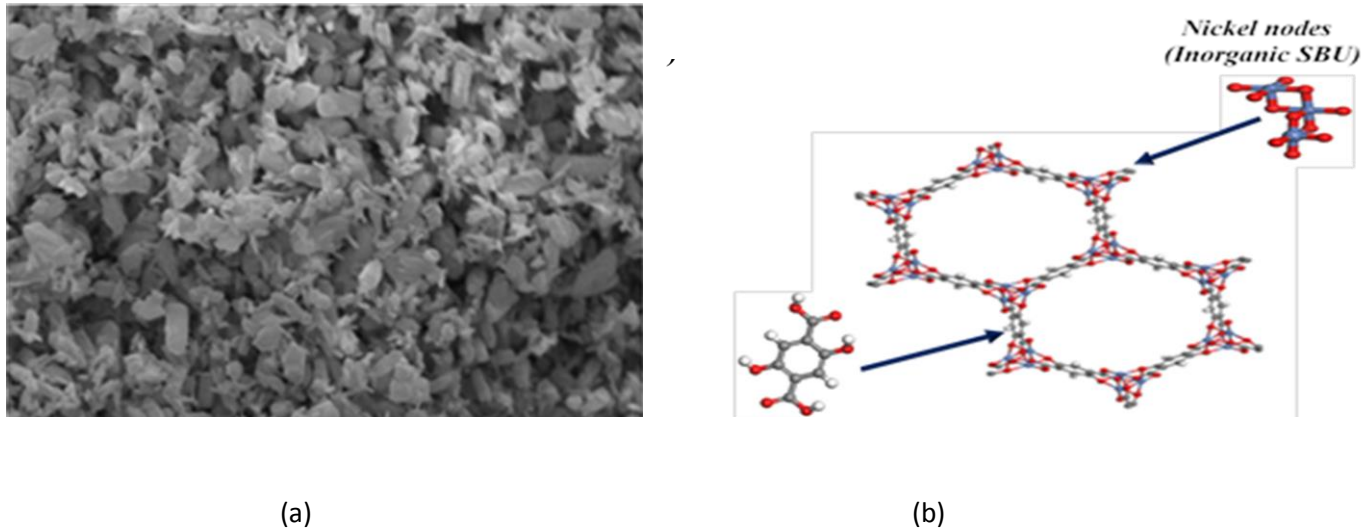


Fig. 4 SEM image (a) and crystal structure (b) for CPO-27Ni

TABLE II
Physical Properties of CPO-27Ni

Property	Value
Pore mean diameter	0.7 nm
Surface area	299 m ² /g
Total Pore volume	217 cm ³ /kg

For prediction of adsorbent material performance, two parameters are required namely adsorption isotherms and kinetics. The maximum amount of adsorbate that can be adsorbed per unit mass of dry material at a certain pressure ratio is called ‘adsorption isotherms’ while the rate of adsorption or desorption at the operating pressure ratio is called ‘adsorption kinetics’. The pressure ratio is defined as the ratio between evaporator to bed pressures during adsorption process or ratio between condenser to bed pressure during desorption process. CPO-27Ni isotherms are modelled using Dubinin-Astakhov (D-A) model (equations 1 & 2) [22] with the constants given in table III [23].

184

$$W^* = W^\infty \exp \left[- \left(\frac{A}{E} \right)^n \right] \quad (1)$$

186 Where W^* is the predicted equilibrium uptake, W^∞ is the adsorbed water vapor mass based on the total
 187 accessible pore volume [$\text{kg}_{\text{ref}}/\text{kg}_{\text{ads}}$], E is the characteristic energy [J/mol], n is an empirical constant and A ,
 188 is the adsorption potential which is given by:

189

$$A = -RT \ln \left(\frac{P}{P_o} \right) \quad (2)$$

191 Where R is the universal gas constant, T is the temperature of the adsorbent material and P/P_o is the partial
 192 pressure ratio.

193

TABLE III
DUBININ-ASTAKHOV EQUATION CONSTANTS

Symbol	Value	Unit ^a
W^∞	0.46826	kg/kg of adsorbent
E	10.0887	kJ/mole
n	5.6476	(-)
R	8314	J/mole.K

^aUnits are; kg = kilogram, K = Kelvin.

194

195 To determine adsorption kinetics, linear driving force (LDF) model commonly used to predict the rate of
 196 adsorption/desorption, (equations 3-4) [24]. Tests using dynamic vapor sorption (DVS) machine have been
 197 carried out at university of Birmingham, UK to determine the relation between uptake and time. By fitting
 198 the test results, the obtained constants of the LDF model are presented in table IV [23].

199

200

$$\frac{dW}{dt} = k(W^* - W) \quad (3)$$

$$k = k_o e^{\left(\frac{-Ea}{RT} \right)} \quad (4)$$

202

TABLE IV
Linear Driving Force, LDF equation constants

Symbol	Pr ^b <0.2	Pr >0.2	Unit ^a
k_o	81.5615	0.7779	1/s
E_a	3.2006E4	1.4806E4	J/mol

^aUnits are; s = second, J = Joule, mol = mole.

^bPr is the pressure ratio between bed and heat exchanger

203

For assessment of adsorption desalination/cooling cycle performance, two parameters are calculated which are Specific Daily Water Production (SDWP) and Specific Cooling Power (SCP). SDWP is the amount of water produced per tonne of adsorbent per day while SCP is the amount of produced cooling per unit mass of adsorbent material used. These parameters are calculated using equations 5-8 [6]:

$$SDWP = \int_0^{t_{cycle}} \frac{Q_{cond} \cdot \tau}{h_{fg} M_a} dt \quad (5)$$

$$SCP = \int_0^{t_{cycle}} \frac{Q_{evap} \cdot \tau}{M_a} dt \quad (6)$$

Where:

$$Q_{cond} = m_{cond} c_p (T_{cond}) (T_{cond,out} - T_{cond,in}) \quad (7)$$

$$Q_{evap} = m_{chilled} c_p (T_{evap}) (T_{chilled,in} - T_{chilled,out}) \quad (8)$$

4. RESULTS AND DISCUSSION

As discussed in section 3, adsorbent material performance depends on the partial pressure ratio determined by the adsorber bed and heat exchanger temperatures. For the material to work at low partial pressure ratio during desorption time ($P(T_{Cond})/P(T_{Des})$), this can be achieved either by increasing the heating fluid temperature or decreasing the condenser cooling water temperature. The operating temperature conditions used in this paper were selected to achieve partial pressure ratios ranging from 0.01 to 0.05 corresponding to condensing temperature ranging from 5°C to 30°C at fixed desorption temperature of 95°C while adsorber bed cooling water is supplied from the mains at average temperature of 15°C. Flowrates of water circuits in evaporator, condenser and adsorber beds are 4, 5 and 15 L/min respectively. Also, this work investigates the effect of other parameters like switching time, cycle time, evaporator water temperature and condenser water temperature on water production and cooling capacity.

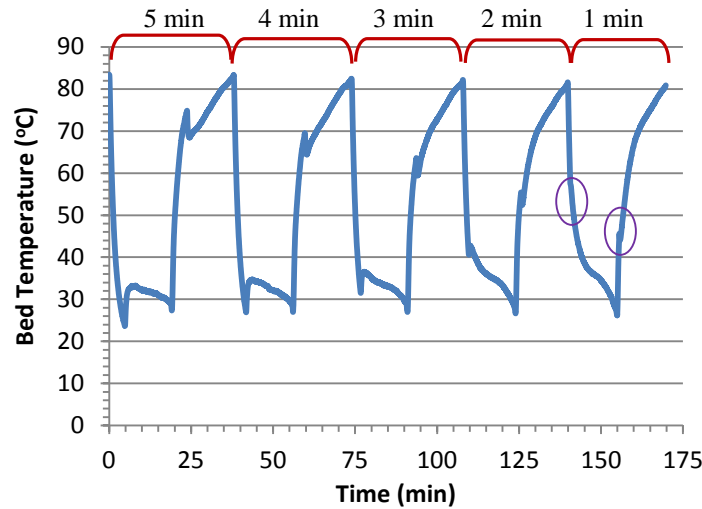
4.1 Switching time effect

Switching time is the period of time when adsorbent bed is not connected neither to the evaporator nor to the condenser. During this time, adsorbent bed is either in precooling or in preheating process to be prepared for adsorption or desorption processes respectively. In this test, five switching times are tested from 5 to 1 min. at constant half cycle time of 14 minutes. Heating and cooling water temperatures are 95°C and 16°C while evaporator and condenser water temperatures are 10°C. Figure 5, shows the adsorber bed temperature through 5 consecutive cycles with switching time decreasing by 1 minute every cycle. It can be seen that as switching time decreases, bed temperature profile becomes more smooth (as indicated

234 by the two circles) leading to reducing the energy demand for heating and cooling the bed. Therefore the
 235 one minute switching time was selected to be the best switching time for all further investigations.

236

237



238

239

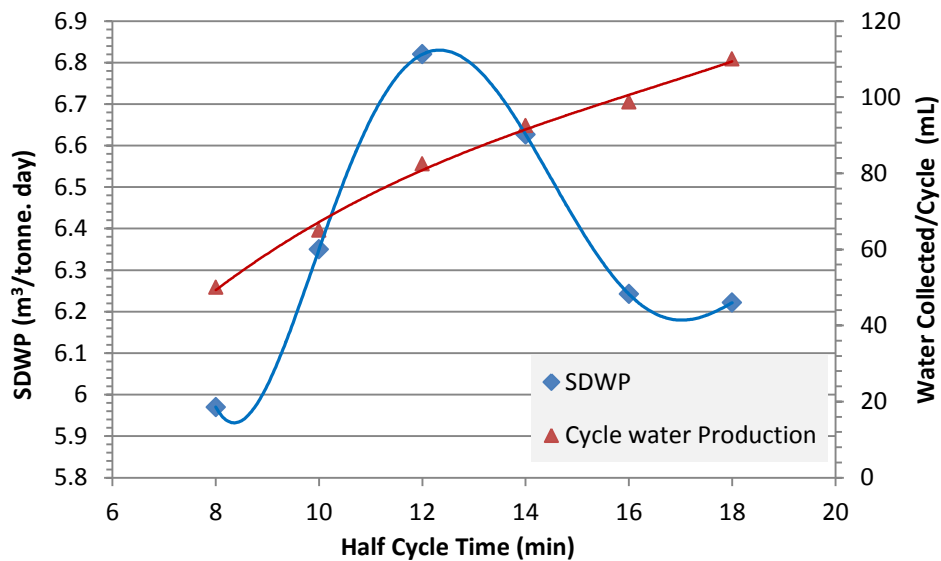
240

Fig. 5 Adsorbent bed temperature through 5 cycles at different switching times

241 4.2 Half cycle time effect

242 Half cycle time is the time for adsorption or desorption processes during the cycle when the bed is either
 243 connected to the evaporator or to the condenser. In this test six half cycle times were investigated ranging
 244 from 8 to 18 minutes and their results are shown in figures 6 & 7.

245



246

247

Fig. 6 SDWP and amount of collected water per cycle at different half cycle times

249

250

251

252

253

254

255

256

257

258

259

260

261

262

263

264

265

266

267

268

269

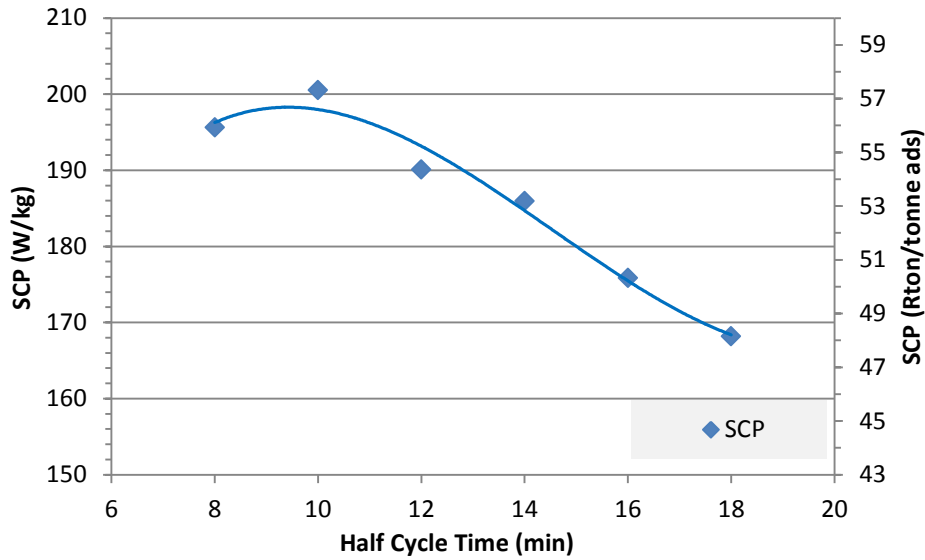


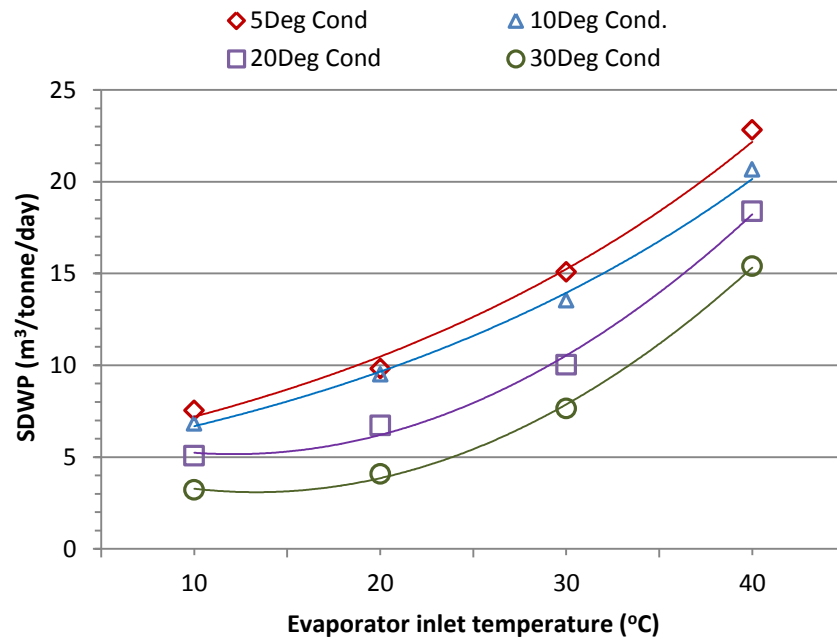
Fig. 7 SCP at different half cycle times

Fig. 6 shows that as the half cycle time increases, the amount of water collected per cycle is increasing. However, by increasing cycle duration, number of cycles per day will decrease which adversely affects the daily water production. Results showed that half cycle time of 12 minutes can produce the maximum amount of daily water production of $6.8\text{m}^3/\text{tonne.day}$. Regarding cooling output, fig. 7 shows that as cycle time increases SCP decreases. This could be attributed to the evaporator temperature profile as it decreases at a higher rate at the beginning than at the end of the adsorption time which results in lower average evaporator temperature at shorter cycle times which in turn increases SCP. Although half cycle time of 10 minutes gives highest SCP of 200 W/kg (57 Rton/tonne.ads), a time of 12 minutes is used for the rest of the experimental work since it results in maximum SDWP which is the main focus of this research.

4.3 Evaporator and Condenser water temperature effect

Water desalination adsorption cycle is an open loop system which is characterized by seawater feed in the evaporator and desalinated fresh water extraction from the condenser. Accordingly, this cycle is unlike closed loop adsorption refrigeration systems which necessitate condenser pressure to be higher than evaporator pressure to allow flowing of the refrigerant from condenser to evaporator [25]. Different evaporator and condenser water inlet temperatures are investigated with the range of $10\text{-}40^\circ\text{C}$ and $5\text{-}30^\circ\text{C}$ respectively. As shown in figures 8 and 9, increasing evaporator water temperature increases daily water production and specific cooling power. In contrast, decreasing condenser temperature increases cycle

270 outputs due to the decrease in the operating partial pressure ratio thus allowing desorption process to reach
 271 low uptakes. By changing evaporator water inlet temperature from 10 to 40°C, water production increases
 272 by 202% from 6.8 to 20.6 m³/tonne adsorbent/day when operating at 10°C condenser. On the other hand,
 273 decreasing condenser water inlet temperature from 30 to 5°C, increases cycle water outputs by 135% from
 274 3.2 to 7.5 m³/tonne adsorbent/day at evaporator temperature of 10°C.
 275 Produced chilled water from the adsorption system can be used for cooling applications like space, process
 276 or district cooling [6]. Figure 9 shows that this system can produce SCP of 225W/kg for evaporator inlet
 277 temperature ranging from 10°C to 20°C suitable for space cooling. Also figure 9 shows that at evaporator
 278 inlet temperature ranging from 30 to 40°C, SCP values can reach 750 W/kg which suitable for process
 279 cooling.



280
 281 Fig. 8 SDWP at different Evaporator and Condenser water temperatures
 282
 283
 284

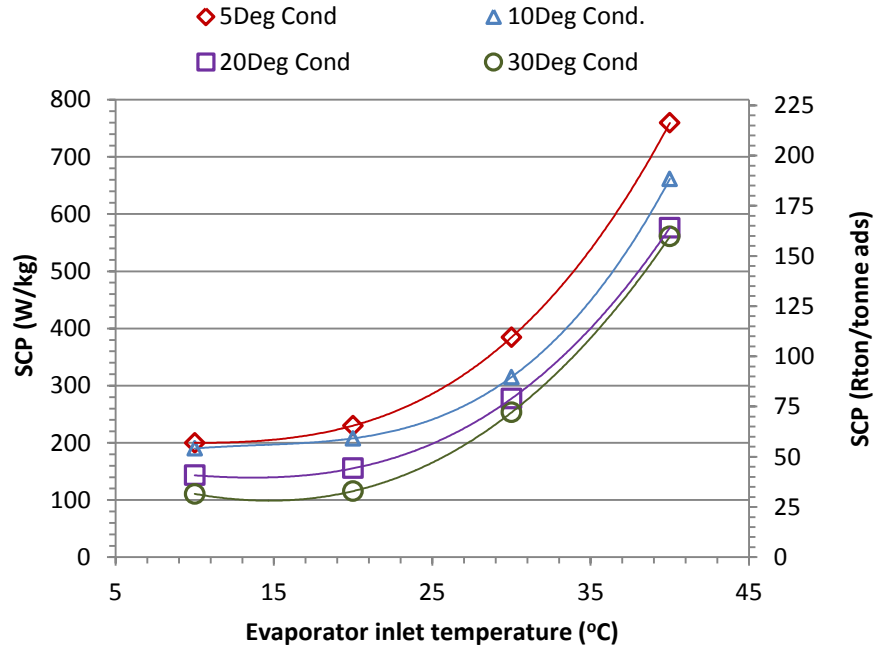


Fig. 9 SCP at different Evaporator and Condenser water temperatures

Figure 10 shows temperature profiles of the main system components at two condenser temperatures of 5 and 30°C while evaporator water inlet temperature is constant at 10°C. Two line groups appear in these figures; the first is denoted by (L) and the other is denoted by (H) which refer to temperature profiles in case of low condenser temperature of 5°C and high condenser temperature of 30°C respectively.

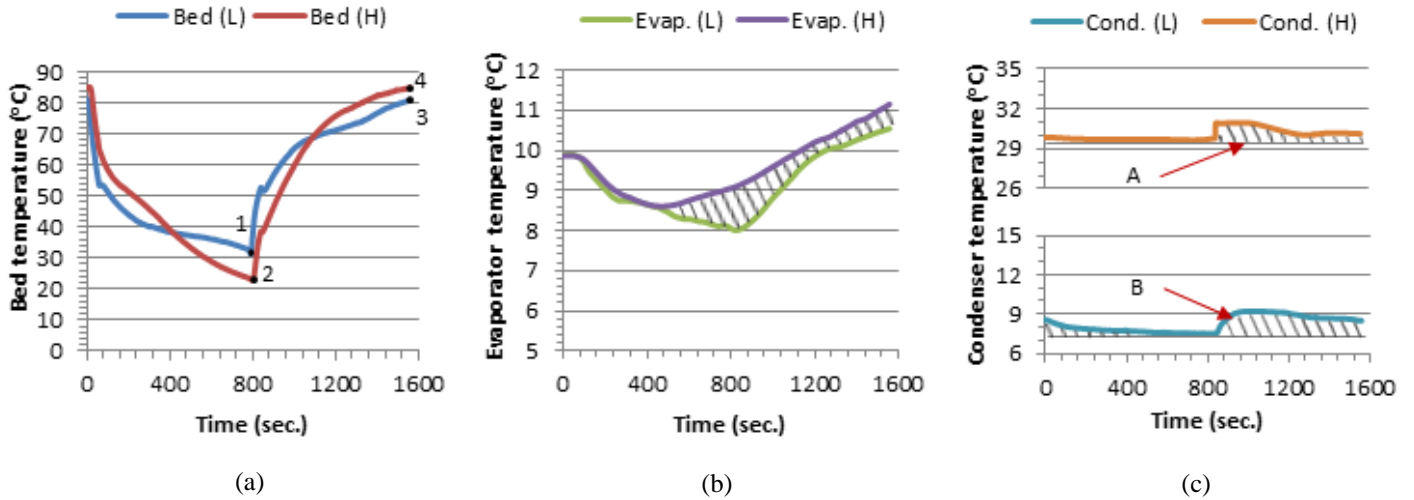


Fig. 10 Temperature profile at two condenser water inlet temperatures, 5°C (L) and 30°C (H)

(a) Adsorber Bed (b) Evaporator (c) Condenser

297

298 As seen in figure 10-a, at lower condenser water inlet temperature of 5°C with higher water production
 299 rates (i.e. higher uptake rate), bed temperature (point 1) cannot reach the low temperature of 22.8°C (point
 300 2) at the end of adsorption process and the high temperature of 84.9°C (point 4) like the case of higher
 301 condenser temperature. This is due to the larger amount of heat released and extracted during adsorption
 302 and desorption processes respectively by the adsorbent material. In figure 10-b the hatched area represents
 303 the increase in cooling effect produced in the evaporator due to decreasing the condenser water inlet
 304 temperature which resulted in low evaporator temperature of 8°C. In contrast, condenser temperature
 305 increases in case of 5°C more than in case of 30°C resulting in area 'B' larger than area 'A', figure 10-c,
 306 which is because of larger amount of water produced at lower condenser water inlet temperature.

307

308 5. NUMERICAL SIMULATION AND VALIDATION

309 A Simulink model has been developed to simulate the adsorption water desalination / cooling system
 310 shown in fig. 1. This model has been validated using the experimental results and then used to predict the
 311 system performance at other operating conditions.

312

313 5.1 Numerical model

314

315 In order to study the cycle, energy equations are solved for evaporator, condenser, adsorber/desorber bed
 316 in addition to mass and salt balance equations for the evaporator [26] as shown in equations 9-13:

317

318 *Evaporator mass balance equation:*

$$319 \frac{dM_{s,evap}}{dt} = \theta \dot{m}_{s,in} - \gamma \dot{m}_b - n \cdot \frac{dW_{ads}}{dt} M_a \quad (9)$$

320

321 *Evaporator salt balance equation:*

$$322 M_{s,evap} \frac{dX_{s,evap}}{dt} = \theta X_{s,in} \dot{m}_{s,in} - \gamma X_{s,evap} \dot{m}_{brine} - n \cdot X_D \frac{dW_{ads}}{dt} M_a \quad (10)$$

323

324 *Evaporator energy balance equation:*

$$325 \left[M_{s,evap} c_{p,s}(T_{evap}, X_{s,evap}) + M_{HX,Evap} c_{p,HX} \right] \frac{dT_{evap}}{dt} = \theta \cdot h_f(T_{evap}, X_{s,evap}) \dot{m}_{s,in} - n \cdot h_{fg}(T_{evap}) \frac{dW_{ads}}{dt} M_a \\ 326 + \dot{m}_{chilled} c_p(T_{evap})(T_{chilled,in} - T_{chilled,out}) \\ 327 - \gamma h_f(T_{evap}, X_{s,evap}) \dot{m}_b \quad (11)$$

Adsorption /desorption bed, energy balance equation:

$$[M_a c_{p,a} + M_{HX} c_{p,HX} + M_{abe} c_{p,abe}] \frac{dT_{ads/des}}{dt} = \pm m_{cw/hw} c_p (T_{cw/hw,in} - T_{cw/hw,out}) \pm z \cdot Q_{st} M_a \frac{dW_{ads/des}}{dt} \quad (12)$$

Where, z is a flag equals 0 in heat recovery phase and 1 in adsorption/desorption phase.

Condenser energy balance equation:

$$[M_{cond} c_p (T_{cond}) + M_{HX,Cond} c_{p,HX}] \frac{dT_{cond}}{dt} = h_f \frac{dM_d}{dt} + h_{fg} (T_{cond}) M_a \left(n \cdot \frac{dW_{des}}{dt} \right) + m_{cond} c_p (T_{cond}) (T_{cond,in} - T_{cond,out}) \quad (13)$$

All energy and mass balance equations in addition to adsorbent characteristics equations (isotherms and kinetics) are solved by Simulink with tolerance value of 1×10^{-6} . In this simulation it was assumed that there is no heat loss from the bed and the temperature of all constituents of each component are kept at the same temperature momentarily.

5.2 Validation of numerical model

Results of an experimental test at the operating conditions described in table I and at evaporator and condenser water temperatures of 10°C were used for validation. Validation of the developed Simulink model is based on a comparison between experimental and numerical temperatures of bed, evaporator and condenser as shown in fig.11 showing good agreement between the experimental and simulation results with an error within $\pm 10\%$ which is presented on table V. Figure 12 compares the experimental and numerical results of daily water production and specific cooling power with an error of 7.3 and 6.3% respectively.

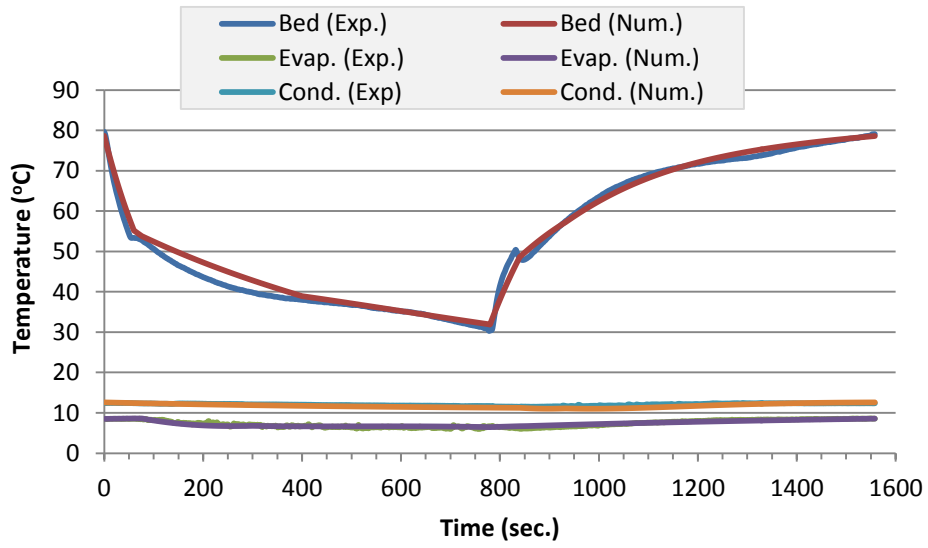


Fig. 11 Comparison of basic cycle components temperatures for numerical and experimental results of a single-Bed adsorption desalination cycle

TABLE V
ERROR RANGE FOR THE VALIDATION OF ADSORPTION
DESALINATION CYCLE

	Maximum (%)	Minimum (%)
<i>Bed 1</i>	7.59	-8.3
<i>Condenser</i>	0.44	-6.1
<i>Evaporator</i>	5.92	-0.69

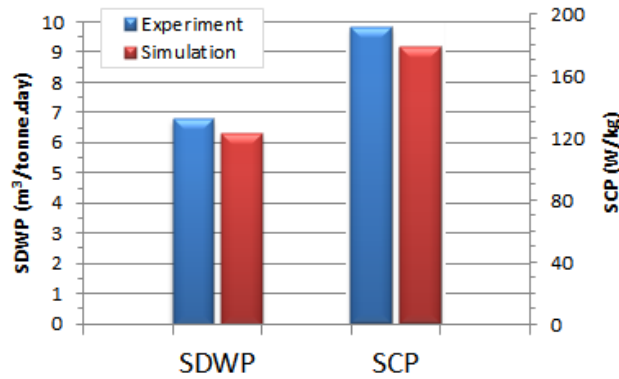


Fig. 12 Comparison of SDWP and SCP for numerical and experimental results for a single-Bed adsorption desalination cycle

The validated mathematical model was used to investigate the system performance at condensing

temperature of 30°C and higher bed heating temperature of 120°C to achieve the same partial pressure as the case used in the model validation above. Figure 13 compares the predicted SDWP and SCP to those produced experimentally at condensing temperature of 10°C and bed heating temperature of 95°C. It can be seen that they are comparable with difference less than 10%. This illustrates that as long as the partial pressure ratio is maintained, the performance of the system will be comparable.

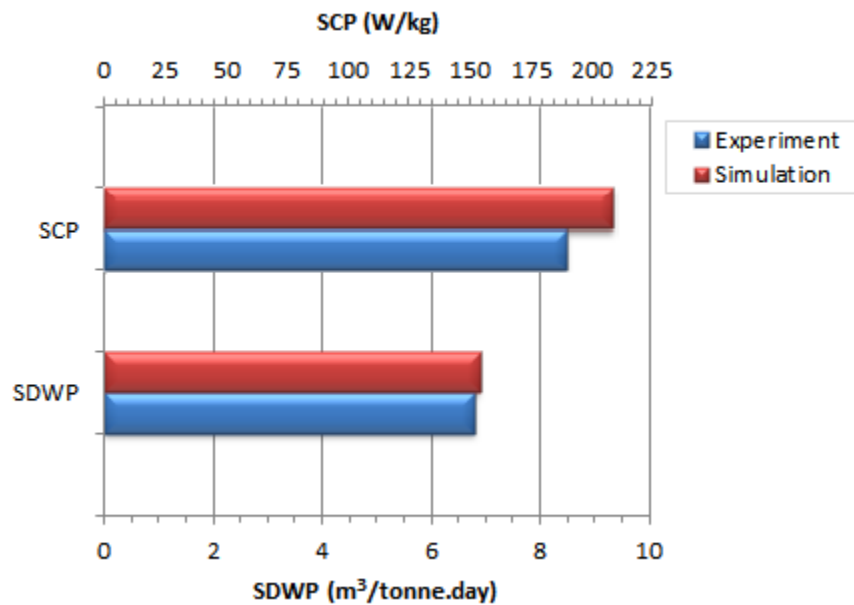


Fig. 13 Comparison of SDWP and SCP for numerical (high desorption and condenser temperatures) and experimental (low desorption and condenser temperatures) results

5.3 Condenser and desorption water temperature effect

SDWP and SCP are shown on figures 14 and 15 respectively at further heating medium inlet temperatures for the range of 110-155°C at different condenser inlet water temperatures ranging from 5 to 30°C. As noticed from experimental results in section 4.3, decreasing condenser water inlet temperature results in more cooling and water production where SDWP and SCP increase by 152% and 95% respectively when condenser water inlet temperature decreases from 30 to 5°C at 110°C desorption temperature. However, increasing desorption temperature enhances cycle outputs as SDWP and SCP are increased by 195% and 96% when desorption temperature increases from 110 to 155°C at the same condenser temperature of 30°C.

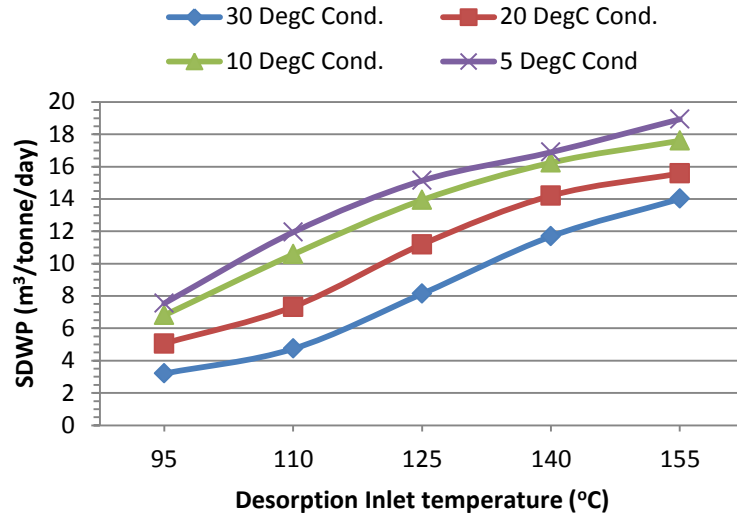


Fig. 14 SDWP at different desorption and condenser water inlet temperatures

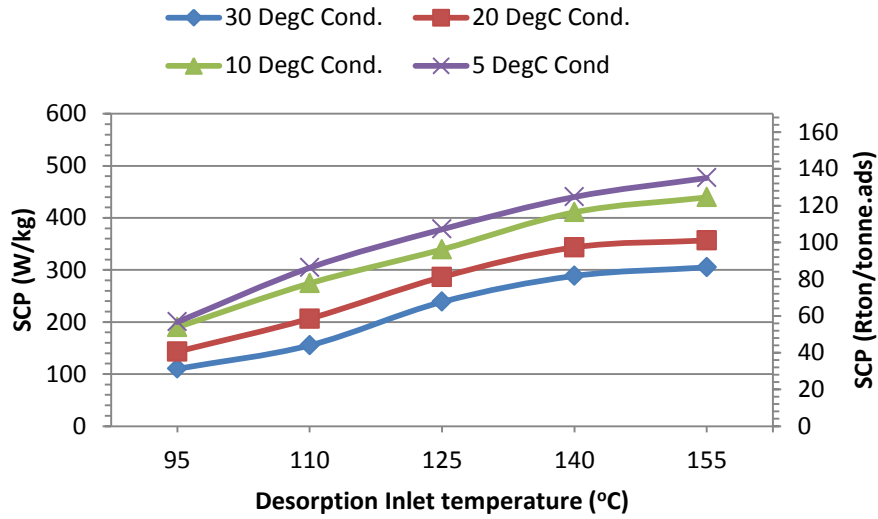


Fig. 15 SCP at different desorption and condenser water inlet temperatures

6. CONCLUSIONS

Adsorption water desalination outperforms conventional desalination technologies in terms of energy consumption, CO₂ emissions and water production cost. MOF is a new class of porous materials with

exceptionally high water adsorption capabilities. CPO-27Ni is a MOF material with higher water uptake value at low partial pressure ratio compared to silica gel leading to advantages in terms of water desalination and cooling production. This work experimentally investigates the use of CPO-27Ni MOF adsorbent material for adsorption desalination/cooling applications. The effect of operating parameters like evaporator and condenser water inlet temperatures, half cycle and switching times on the system performance in terms of specific daily water production and specific cooling power were investigated. It was shown that a maximum water production of 22.8 m³/tonne.day was achieved as well as cooling of 215.9 Rton/tonne adsorbent at maximum evaporator water inlet temperature of 40°C and condenser water inlet temperature of 5°C. This is due to the nature of the isotherm curve of CPO-27Ni and the fact that reducing condenser temperature and increasing evaporator temperature, maximizes the cycle uptake and hence results in more cooling and water outputs. In addition, a numerical model was developed and validated using the experimental results and then used to predict cycle performance at other operating conditions. From this model, it was concluded that as long as the partial pressure ratio is maintained, the same cycle outputs could be obtained using different combinations between condenser and desorption temperatures.

7. ACKNOWLEDGEMENT

The authors would like to thank Weatherite Holdings ltd. for sponsoring the project.

REFERENCES

- [1] H. Ettouney. Seawater Desalination, Conventional and Renewable Energy Processes: Springer; 2009.
- [2] P. G. Youssef, R. K. Al-Dadah, S. M. Mahmoud. Comparative Analysis of Desalination Technologies. Energy Procedia. 2014;61:2604-7.
- [3] T. Mezher, H. Fath, Z. Abbas, A. Khaled. Techno-economic assessment and environmental impacts of desalination technologies. Desalination. 2011;266:263-73.
- [4] K. Thu. Adsorption desalination Theory and experiment: National University of Singapore; 2010.
- [5] J. W. Wu, E. J. Hu, M. J. Biggs. Thermodynamic cycles of adsorption desalination system. Applied Energy. 2012;90:316-22.
- [6] K. C. Ng, K. Thu, B. B. Saha, A. Chakraborty. Study on a waste heat-driven adsorption cooling cum desalination cycle. International Journal of Refrigeration. 2012;35:685-93.
- [7] A. Chakraborty, K. Thu, K. C. Ng. Advanced Adsorption Cooling Cum Desalination Cycle- a Thermodynamic Framework. ASME 2011 International Mechanical Engineering Congress & Exposition IMECE2011. Denver, Colorado, USA2011.
- [8] K. C. Ng, K. Thu, A. Chakraborty, B. B. Saha, W. G. Chun. Solar-assisted dual-effect adsorption cycle for the production of cooling effect and potable water. International Journal of Low-Carbon Technologies. 2009;4:61-7.
- [9] J. W. Wu, M. J. Biggs, E. J. Hu. Thermodynamic analysis of an adsorption-based desalination cycle. Chemical Engineering Research and Design. 2010;88:1541-7.
- [10] T. X. Li, R. Z. Wang, H. Li. Progress in the development of solid-gas sorption refrigeration thermodynamic cycle driven by low-grade thermal energy. Progress in Energy and Combustion Science. 2014;40:1-58.
- [11] X. Wang, K. C. Ng. Experimental investigation of an adsorption desalination plant using low-temperature waste heat. Applied Thermal Engineering. 2005;25:2780-9.

- [12] K. C. Ng, X.-L. Wang, L. Gao, A. Chakraborty, B. B. Saha, S. Koyama, A. Akisawa, T. Kashiwagi. Apparatus and Method for Desalination. 2010.
- [13] K. Thu, K. C. Ng, B. B. Saha, A. Chakraborty, S. Koyama. Operational strategy of adsorption desalination systems. *International Journal of Heat and Mass Transfer*. 2009;52:1811-6.
- [14] S. Mitra, P. Kumar, K. Srinivasan, P. Dutta. Performance evaluation of a two-stage silica gel + water adsorption based cooling-cum-desalination system. *International Journal of Refrigeration*. 2015.
- [15] P. G. Youssef, S. M. Mahmoud, R. K. Al-Dadah. Effect of Evaporator Temperature on the Performance of Water Desalination / Refrigeration Adsorption System Using AQSOA-ZO2. *International Journal of Environment, Chemical, Ecological, Geological Engineering*. 2015;9:679-83.
- [16] P. G. Youssef, S. M. Mahmoud, R. K. Al-Dadah. Numerical simulation of combined adsorption desalination and cooling cycles with integrated evaporator/condenser. *Desalination*. 2016;392:14-24.
- [17] S. M. Ali, A. Chakraborty. Adsorption assisted double stage cooling and desalination employing silica gel+water and AQSOA-ZO2+water systems. *Energy Conversion and Management*. 2016;117:193-205.
- [18] E. Elsayed, R. Al-Dadah, S. Mahmoud, A. Elsayed, P. A. Anderson. Aluminium fumarate and CPO-27(Ni) MOFs: Characterization and Thermodynamic Analysis for Adsorption Heat Pump Applications. *Applied Thermal Engineering*. 2016;99:802-12.
- [19] A. Elsayed, R. AL-Dadah, S. Mahmoud, B. Shi, P. Youssef, A. Elshaer, W. Kaialy. Characterisation of CPO-27Ni Metal Organic Framework Material for Water Adsorption. *SUSTEM International Conference. Newcastle Upon Tyne* 2015. p. 284-90.
- [20] A. Elsayed, E. Elsayed, R. Al-Dadah, S. Mahmoud, A. Elshaer, W. Kaialy. Thermal energy storage using metal–organic framework materials. *Applied Energy*. 2016.
- [21] E. Elsayed, R. Al-Dadah, S. Mahmoud, P. A. Anderson, A. Elsayed, P. G. Youssef. CPO-27(Ni), aluminium fumarate and MIL-101(Cr) MOF materials for adsorption water desalination. *Desalination*. 2016.
- [22] S. K. Henninger, M. Schick Tanz, P. P. C. Hügenell, H. Sievers, H. M. Henning. Evaluation of methanol adsorption on activated carbons for thermally driven chillers part I: Thermophysical characterisation. *International Journal of Refrigeration*. 2012;35:543-53.
- [23] B. Shi, R. Al-Dadah, S. Mahmoud, A. Elsayed, E. Elsayed. CPO-27(Ni) metal–organic framework based adsorption system for automotive air conditioning. *Applied Thermal Engineering*. 2016;106:325-33.
- [24] L. X. Gong, R. Z. Wang, Z. Z. Xia, C. J. Chen. Design and performance prediction of a new generation adsorption chiller using composite adsorbent. *Energy Conversion and Management*. 2011;52:2345-50.
- [25] J. W. Wu, M. J. Biggs, P. Pendleton, A. Badalyan, E. J. Hu. Experimental implementation and validation of thermodynamic cycles of adsorption-based desalination. *Applied Energy*. 2012;98:190-7.
- [26] K. C. Ng, K. Thu, Y. Kim, A. Chakraborty, G. Amy. Adsorption desalination: An emerging low-cost thermal desalination method. *Desalination*. 2013;308:161-79.